



$(g - 2)_{e,\mu}$ ANOMALIES AND LEPTON FLAVOR VIOLATING DECAYS IN
A TWO HIGGS DOUBLET MODEL: INVERTED ORDER SCHEME OF
NEUTRINO OSCILLATION DATA

Nguyen Hua Thanh Nha^{1,2}, Le Ngoc Quyen³, Lam Thi Thanh Phuong^{4,5,6}, Nguyen Thi Cam Nhungh⁷,
Nguyen Thanh Phong⁴, Vu Quang Tho⁸, Trinh Thi Hong^{5,6,*}

¹ Subatomic Physics Research Group, Science and Technology Advanced Institute, Van Lang University,
Ho Chi Minh City, Vietnam

² Faculty of Applied Technology, School of Engineering and Technology, Van Lang University, Ho Chi
Minh City, Vietnam

³ Mang Thit High School, Hamlet 1, Cai Nhum Ward, Mang Thit District, Vinh Long Province, Vietnam

⁴ Can Tho University, 3/2 Street, Can Tho City, Vietnam

⁵ An Giang University, Long Xuyen City, Vietnam

⁶ Vietnam National University, Ho Chi Minh City, Vietnam

⁷ No. 126 Nguyen Thien Thanh Street, Ward 5, Tra Vinh City, Vietnam

⁸ Tan Trao University, Km 6, Trung Mon, Yen Son District, Tuyen Quang Province, Vietnam

*Email address: tthong@agu.edu.vn

<http://doi.org/10.51453/2354-1431/2024/1174>

Article info

Received:

18/7/2024

Revised:

15/8/2024

Accepted:

25/8/2024

Keywords:

Higgs boson decay, FLV decay, 2HDM.

Abstract:

The lepton flavor violating decays $h \rightarrow e_b^\pm e_a^\mp$, $Z \rightarrow e_b^\pm e_a^\mp$, and $e_b \rightarrow e_a \gamma$ in a two-Higgs-doublet model have been discussed in (T. T. Hong *et al*, 2024). Still, only the normal order (NO) scheme of the neutrino oscillation data was used for numerical investigation. In this work, we will show numerical results corresponding to the inverted order (IO) scheme and compare them with those predicted by the NO scheme. In addition, we focus on the dependence of all lepton flavor violating decays as functions of the heaviest active neutrino masses, which was not shown in detail previously. Our results confirm the consistency with a recent work (T. T. Hong *et al*, 2024) in all allowed values of the heaviest active neutrino mass.



MOMENT TỪ DỊ THƯỜNG ($g - 2$) _{e,μ} VÀ CÁC QUÁ TRÌNH RÃ VI PHẠM SỐ LEPTON THẾ HỆ TRONG MÔ HÌNH HAI LUỒNG TUYỀN HIGGS: TRƯỜNG HỢP NEUTRINO PHÂN BẬC NGHỊCH

Nguyễn Hứa Thanh Nhã^{1,2}, Lê Ngọc Quyên³, Lâm Thị Thanh Phương^{4,5}, Nguyễn Thị Cẩm Nhung⁶, Nguyễn Thanh Phong⁴, Vũ Quang Thọ⁷, Trịnh Thị Hồng^{5,*}

¹ Nhóm nghiên cứu Vật lý hạt hạ nguyên tử, Viện Tiên tiến Khoa học và Công nghệ, Trường Đại học Văn Lang, Việt Nam

² Khoa Công nghệ ứng dụng, Trường Đại học Văn Lang, Việt Nam

³ Trường THPT Mang Thít, Khóm 1, Thị Trấn Cái Nhum, Huyện Mang Thít, Tỉnh Vĩnh Long, Việt Nam

⁴ Trường Đại học Cần Thơ, Việt Nam

⁵ Trường Đại học An Giang, ĐHQG-HCM, Việt Nam

⁶ Trường Đại học Trà Vinh, Việt Nam

⁷ Trường Đại học Tân Trào, Việt Nam

*Email address: tthong@agu.edu.vn

<http://doi.org/10.51453/2354-1431/2024/1174>

Thông tin bài viết

Ngày nhận bài:

18/7/2024

Ngày hoàn thiện:

15/8/2024

Ngày chấp nhận:

25/8/2024

Từ khóa:

Rã boson Higgs, Rã vi phạm số lepton thế hệ, Mô hình hai luồng tuyển Higgs.

Tóm tắt:

Các quá trình rã vi phạm số lepton thế hệ (LFV) $h \rightarrow e_b^\pm e_a^\mp$, $Z \rightarrow e_b^\pm e_a^\mp$, và $e_b \rightarrow e_a \gamma$ trong mô hình Hai luồng tuyển Higgs đã được thảo luận trong một nghiên cứu gần đây của chúng tôi (T. T. Hong *et al*, 2024). Tuy nhiên, chúng tôi chỉ mới khảo sát số cho trường hợp neutrino phân bậc thuận (NO) từ dữ liệu thực nghiệm về dao động neutrino. Do đó, trong bài báo này, chúng tôi sẽ khảo sát thêm trường hợp còn lại - trường hợp neutrino phân bậc nghịch (IO) và so sánh chúng với các dự đoán từ trường hợp NO. Ngoài ra, chúng tôi tập trung khảo sát sự phụ thuộc của tất cả các quá trình rã LFV như là các hàm của khối lượng neutrino hoạt động nặng nhất, điều này chưa được trình bày chi tiết trước đó. Kết quả chúng tôi thu được xác nhận tính nhất quán với công trình trước đó (T. T. Hong *et al*, 2024) trong tất cả các giá trị được phép của khối lượng neutrino hoạt động nặng nhất.

1 INTRODUCTION

The Standard Model (SM) of particle physics is to this day an accurate description of the elementary particles and their interactions. Nevertheless, there are still problems that the SM cannot explain, such as the lepton flavor violating (LFV) decays, the origin of the neutrino mass and the lep-

ton flavour violation in the neutrino sector, charged lepton anomalies ($g - 2$) _{e,μ} . Besides, neutrino oscillation experiments have shown it has mass and mixing flavours. Therefore, expanding the SM with the Beyond the SM (BSM) theories is indispensable work. A recent work (T. T. Hong *et al*, 2024) studied all LFV decay satisfying two experimental data of ($g - 2$) anomalies, namely

- The latest data of $a_\mu \equiv (g - 2)_\mu / 2$ was given in (Aguillard, D. P. et al. [Muon g-2], 2023), which shows a clear discrepancy from the SM prediction of $a_\mu^{\text{SM}} = 116591810(43) \times 10^{-11}$ (Aoyama, T. et al., 2020). The deviation between experiment and SM prediction used here is

$$\Delta a_\mu^{\text{NP}} \equiv a_\mu^{\text{exp}} - a_\mu^{\text{SM}} = (2.49 \pm 0.48) \times 10^{-9} (5.1\sigma). \quad (1)$$

- Similarly, the discrepancy between experimental and SM for $(g - 2)_e$ data is:

$$\Delta a_e^{\text{NP}} \equiv a_e^{\text{exp}} - a_e^{\text{SM}} = (3.4 \pm 1.6) \times 10^{-13}, \quad (2)$$

where a_e^{exp} corresponds to the recent experimental data given in (Fan, X., Myers, T. G., Sukra, B. A. D., Gabrielse, G. , 2023).

- The decay rates such as charged LFV (cLFV), LFV Higgs (LFVh) decays, and LFV Z-boson (LFVZ) decays are constrained experimentally given in the Table 1 (Aubert, Bernard et al. [BaBar], 2010; Baldini, A. M. et al. [MEG], 2016; Abdesselam, A. et al. [Belle], 2021).

	Branching ratio (Br)	Most recent	Future sensitivity
cLFV	$\text{Br}(\tau \rightarrow \mu\gamma)$	$< 4.4 \times 10^{-8}$ (Aubert, Bernard et al. [BaBar], 2010; Baldini, A. M. et al. [MEG], 2016; Abdesselam, A. et al. [Belle], 2021)	$< 6.9 \times 10^{-9}$ (Baldini, A. M. et al. [MEG II], 2018; Altmannshofer, W. et al. [Belle-II], 2020)
	$\text{Br}(\tau \rightarrow e\gamma)$	$< 3.3 \times 10^{-8}$ (Aubert, Bernard et al. [BaBar], 2010; Baldini, A. M. et al. [MEG], 2016; Abdesselam, A. et al. [Belle], 2021)	$< 9.0 \times 10^{-9}$ (Baldini, A. M. et al. [MEG II], 2018; Altmannshofer, W. et al. [Belle-II], 2020)
	$\text{Br}(\mu \rightarrow e\gamma)$	$< 4.2 \times 10^{-13}$ (Aubert, Bernard et al. [BaBar], 2010; Baldini, A. M. et al. [MEG], 2016; Abdesselam, A. et al. [Belle], 2021)	$< 6 \times 10^{-14}$ (Baldini, A. M. et al. [MEG II], 2018; Altmannshofer, W. et al. [Belle-II], 2020)
LFVh	$\text{Br}(h \rightarrow \tau\mu)$	$< 1.5 \times 10^{-3}$ (Sirunyan, A. M. et al. [CMS], 2021)	orders of $\mathcal{O}(10^{-4})$ (Qin, Q. et al. 2018; Barman, R. K., Dev, P. S. B., Thapa, A., 2023; Aoki, M., Kanemura, S., Takeuchi, M., Zamakhsyari, L., 2023)
	$\text{Br}(h \rightarrow \tau e)$	$< 2.2 \times 10^{-3}$ (Sirunyan, A. M. et al. [CMS], 2021)	orders of $\mathcal{O}(10^{-4})$ (Qin, Q. et al. 2018)
	$\text{Br}(h \rightarrow \mu e)$	$< 6.1 \times 10^{-5}$ (Aad, G. et al. [ATLAS], 2020)	orders of $\mathcal{O}(10^{-5})$ (Qin, Q. et al. 2018)
LFVZ	$\text{Br}(Z \rightarrow \tau^\pm \mu^\mp)$	$< 6.5 \times 10^{-6}$ (Aad, G. et al. [ATLAS], 2022)	10^{-6} at HL-LHC (Dam, M., 2019) and 10^{-9} at FCC-ee (Dam, M., 2019; Abada, A. et al. [FCC], 2019)
	$\text{Br}(Z \rightarrow \tau^\pm e^\mp)$	$< 5.0 \times 10^{-6}$ (Aad, G. et al. [ATLAS], 2022)	10^{-6} at HL-LHC (Dam, M., 2019) and 10^{-9} at FCC-ee (Dam, M., 2019; Abada, A. et al. [FCC], 2019)
	$\text{Br}(Z \rightarrow \mu^\pm e^\mp)$	2.62×10^{-7} (Aad, G. et al. [ATLAS], 2023)	7×10^{-8} at HL-LHC (Aad, G. et al. [ATLAS], 2022) and 10^{-10} at FCC-ee (Dam, M., 2019); Abada, A. et al. [FCC], 2019)

Table 1. The latest experimental constraints and future sensitivity of Brs in the cLFV, LFVh, and LFVZ decay processes.

Our work is arranged as follows. In section 2, we will investigate the three LFV decay classes, namely $e_b \rightarrow e_a \gamma$, $Z \rightarrow e_b^\pm e_a^\mp$, and $h \rightarrow e_b^\pm e_a^\mp$ in the 2HDM $N_{L,R}$ framework, concentrating on the regions of the parameter space accommodating the 1σ range of the $(g - 2)_{e,\mu}$ experimental data. The numerical investigation will be shown in Sec. 3, where we focus on the dependence of LFV decay rates on the heaviest active neutrino masses. Finally, we summarize important results in the section conclusion.

2 THE 2HDM WITH INVERSE SEESAW NEUTRINOS

2.1 Particle content and couplings

In this work, we will study the model discussed in (T. T. Hong *et al*, 2024) discussed recently to explain experimental data of $(g - 2)_{e,\mu}$ anomalies, where all LFV processes mentioned above will be discussed, namely the particle content is of the leptons and Higgs sector is listed in Table 2, which is a particular model (2HDM $N_{L,R}$) mentioned in (Hue, L. T. *et al*, 2023).

The quark sector is omitted, see reviews in (Mondal, T., Okada, H., 2022; Branco, G. C. *et al*, 2012).

The Yukawa Lagrangian of leptons is (Mondal, T., Okada, H., 2022)

$$\begin{aligned} -\mathcal{L}_Y = & \overline{L_L} y_\ell H_1 e_R + \overline{L_L} f \tilde{H}_2 N_R + \overline{N_L} y^\chi e_R \chi^+ \\ & + \overline{N_L} y_N N_R \varphi + \frac{(N_L)^C}{\Lambda} \frac{\lambda_L}{\Lambda} N_L \varphi^2 + \text{h.c.}, \end{aligned} \quad (3)$$

where $\tilde{H}_2 = i\sigma_2 H_2^*$, y_ℓ , f , Y_N , y^χ , and λ_L are 3×3 matrices respectively correspond to $y_{\ell,ab}$, f_{ab} , g_{ab} , and $\lambda_{L,ab}$ with $a, b = 1, 2, 3$. The five-dimension effective matrix μ_L generates small Majorana values consistent with the ISS form.

Regarding to the LFV decays, including LFV h ,

Symmetry	L_L	e_R	N_L	N_R	H_1	H_2	φ	χ^-
$SU(3)_C$	1	1	1	1	1	1	1	1
$SU(2)_L$	2	1	1	1	2	2	1	1
$U(1)_Y$	$-\frac{1}{2}$	-1	0	0	$\frac{1}{2}$	$\frac{1}{2}$	0	-1
\mathbb{Z}_2	-	-	+	+	-	+	+	-

Table 2. Particle content of the 2HDM $N_{L,R}$

LFVZ, and cLFV decays. All needed formulas for decay rates $\text{Br}(h \rightarrow e_b e_a)$, $\text{Br}(Z \rightarrow e_b e_a)$, and $\text{Br}(e_b \rightarrow e_a \gamma)$ were determined in (T. T. Hong *et al*, 2024), therefore we do not repeat here. We just focus on the main ingredients to establish the IO scheme for numerical investigation.

The branching ratios of the cLFV decays are formulated as follows (Lavoura, L., 2003; Hue, L. T., Ninh, L. D., Thuc, T. T., Dat, N. T. T., 2018; Crivellin, A., Hoferichter M., Schmidt-Wellenburg, P., 2018):

$$\begin{aligned} \text{Br}(e_b \rightarrow e_a \gamma) = & \frac{48\pi^2}{G_F^2 m_b^2} \left(|c_{(ab)R}|^2 + |c_{(ba)R}|^2 \right) \\ & \times \text{Br}(e_b \rightarrow e_a \bar{\nu}_a \nu_b), \end{aligned} \quad (4)$$

where $G_F = g^2/(4\sqrt{2}m_W^2)$, $\text{Br}(\mu \rightarrow e \bar{\nu}_e \nu_\mu) \simeq 1$, $\text{Br}(\tau \rightarrow e \bar{\nu}_e \nu_\tau) \simeq 0.1782$, $\text{Br}(\tau \rightarrow \mu \bar{\nu}_\mu \nu_\tau) \simeq 0.1739$ (Workman, R. L. *et al* [Particle Data Group], 2022), and all relevant analytic formulas were given in detail in previous research (T. T. Hong *et al*, 2024). We only comment here on important relating to the IO scheme of the neutrino oscillation data that is necessary for numerical investigation in this work. The non-zero values of $c_{(ab)R}$ and $c_{(ba)R}$ with $b \neq a$ may give large contributions to the cLFV rates, especially the main contribution to a_{e_a} is from the two singly charged Higgs boson c_k^\pm , denoted as $a_{e_a,0}(c^\pm)$ expressed by the following analytic formula

$$a_{e_a,0}(c^\pm) = \frac{G_F m_a^2}{\sqrt{2}\pi^2} \times \text{Re} \left\{ \left[\frac{vt_\beta^{-1} c_\alpha s_\alpha}{\sqrt{2}m_a} U_{\text{PMNS}} \hat{x}_\nu^{1/2} y^\chi \right]_{aa} \right. \\ \left. \times [x_1 f_\Phi(x_1) - x_2 f_\Phi(x_2)] \right\} \quad (5)$$

with $x_k = M_0^2/m_{c_k}^2$ and

$$\hat{x}_\nu \equiv \frac{\hat{m}_\nu}{\mu_0} = x_0 \times \text{diag} \left(\frac{m_{n_1}}{m_{n_2}}, 1, \frac{m_{n_3}}{m_{n_2}} \right), \quad x_0 \equiv \frac{m_{n_2}}{\mu_0}. \quad (6)$$

This formula with $b \neq a$ will result in unacceptable values of cLFV decay rates excluded by recent experimental constraints. According to this discussion, $c_{(ab)R,0}$ will be chosen in the diagonal form to derive the Yukawa coupling matrix y^χ at the beginning of our numerical investigation

$$c_{(ab)R,0} \propto \left[U_{\text{PMNS}} \hat{x}_\nu^{1/2} y^\chi \right]_{ab} \propto \delta_{ab}. \quad (7)$$

In particular, y^χ is derived in terms of a diagonal matrix y^d defined as follows:

$$\begin{aligned} & U_{\text{PMNS}} \times \text{diag} \left(\frac{m_{n_1}}{m_{n_2}}, 1, \frac{m_{n_3}}{m_{n_2}} \right)^{1/2} y^\chi \\ &= y^d \equiv \text{diag}(y_{11}^d, y_{22}^d, y_{33}^d), \end{aligned} \quad (8)$$

where $m_{n_3} < m_{n_1} < m_{n_2}$ with respect to the inverted order of the neutrino oscillation data will be selected in the numerical examination. We emphasize that Eq.(8) was defined for the IO scheme, which is completely different from the NO scheme with $m_{n_1} < m_{n_2} < m_{n_3}$ mentioned previously in (T. T. Hong *et al.*, 2024). In contrast, the analytic formulas for main contribution $a_{e_a,0}$ is the same as that given in (Hue, L. T., Cárcamo Hernández, A. E., Long, H. N., Hong, T. T., 2022)

$$\begin{aligned} a_{e_a,0} = & \frac{G_F m_a^2 \sqrt{x_0}}{\sqrt{2}\pi^2} \times \text{Re} \left[\frac{v t_\beta^{-1} c_\alpha s_\alpha}{\sqrt{2} m_a} y^d \right]_{aa} \\ & \times [x_1 f_\Phi(x_1) - x_2 f_\Phi(x_2)], \end{aligned} \quad (9)$$

while formulas with m_{n_3} must be replaced with m_{n_2} , especially the quantity

$$x_0 \equiv \frac{m_{n_2}}{\mu_0} \quad (10)$$

defining the ratio between the active neutrino mass and the ISS scale μ_0 . To be consistent with the right experimental ranges of $(g-2)_{e,\mu}$, it was shown that x_0 must be large enough, namely $x_0 > \mathcal{O}(10^{-7})$.

3 NUMERICAL DISCUSSION FOR THE IO SCHEME

In the IO scheme corresponding to $m_{n_3} < m_{n_1} < m_{n_2}$, we choose experimental data as follows

(Workman, R. L. *et al.* [Particle Data Group], 2022)

$$\begin{aligned} s_{12}^2 &= 0.318^{+0.016}_{-0.016}, \quad s_{23}^2 = 0.578^{+0.017}_{-0.010}, \\ s_{13}^2 &= 2.225^{+0.064}_{-0.070} \times 10^{-2}, \quad \delta = 284^{+26}_{-28} [\text{Deg}], \\ \Delta m_{21}^2 &= 7.5^{+0.22}_{-0.20} \times 10^{-5} [\text{eV}^2], \\ \Delta m_{32}^2 &= -2.52^{+0.03}_{-0.02} \times 10^{-3} [\text{eV}^2]. \end{aligned} \quad (11)$$

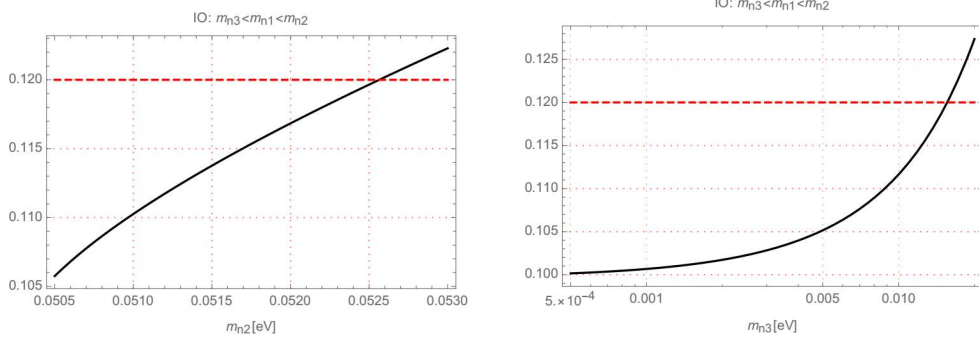
The active mixing matrix and neutrino masses are determined below

$$\begin{aligned} \hat{m}_\nu &= (\hat{m}_\nu^2)^{1/2} \\ &= \text{diag} \left(\sqrt{m_{n_2}^2 - \Delta m_{21}^2}, m_{n_2}, \sqrt{m_{n_2}^2 + \Delta m_{32}^2} \right), \\ U_{\text{PMNS}} &= \\ &\begin{pmatrix} 0.817 & 0.558 & 0.036 + 0.145i \\ -0.389 + 0.091i & 0.521 + 0.062i & 0.752 \\ 0.409 + 0.078i & -0.641 + 0.053i & 0.642 \end{pmatrix} \end{aligned} \quad (12)$$

where U_{PMNS} is chosen at the best-fit point, while three active neutrino masses are functions of m_{n_2} —the heaviest. In addition, values of m_{n_2} must satisfy two conditions including the constraint from Plank2018 (Aghanim, N. *et al.* [Planck], 2020) that $\sum_{a=1}^3 m_{n_a} \leq 0.12$ eV and $m_{n_2}^2 \geq |\Delta m_{32}^2|$ derived from Eq.(12), leading to the allowed range of the heaviest $m_{n_2} \in [0.0505, 0.0526]$ eV. The dependence of the sum of three active neutrinos on different neutrino masses is shown in Fig. 1, where the left (right) panel relates to m_{n_2} (m_{n_3}). We can see that m_{n_3} can small down to the zero value. While the respective maximal one is about 0.015 eV. Because if we use m_{n_3} as a variable to investigate, the Eq.(8) will be more difficult to define the inverse matrix with one zero diagonal entry. Therefore, we will choose m_{n_2} for convenience in numerical investigation. The non-unitary of the active neutrino mixing matrix $(I_3 - \frac{1}{2}RR^\dagger)U_{\text{PMNS}}$ is constrained very strictly by $\eta \equiv \frac{1}{2}|RR^\dagger| \propto \hat{x}_\nu \propto x_0$ in the ISS framework (Mondal, T., Okada, H., 2022).

The well-known numerical parameters are (Workman, R. L. *et al.* [Particle Data Group], 2022)

$$\begin{aligned} g &= 0.652, \quad G_F = 1.1664 \times 10^{-5} \text{ GeV}, \quad s_W^2 = 0.231, \\ \alpha_e &= 1/137, \quad e = \sqrt{4\pi\alpha_e}, \quad m_W = 80.377 \text{ GeV}, \\ m_Z &= 91.1876 \text{ GeV}, \quad m_h = 125.25 \text{ GeV}, \\ \Gamma_h &= 4.07 \times 10^{-3} \text{ GeV}, \quad \Gamma_Z = 2.4955 \text{ GeV}, \\ m_e &= 5 \times 10^{-4} \text{ GeV}, \quad m_\mu = 0.105 \text{ GeV}, \\ m_\tau &= 1.776 \text{ GeV}. \end{aligned} \quad (13)$$



Figuer 1. The sum of three neutrino masses as functions of the heaviest (lightest) mass in the left (right) panel. The dashed-red line shows the upper bound from Plank 2018 results (Aghanim, N. et al. [Planck], 2020).

To constrain effectively the most strict allowed ranges of entries of the matrix y^d , we release some conditions to determine the crude allowed ranges. Firstly, the most strict experimental constraint of $\text{Br}(\mu \rightarrow e\gamma)$ results in the suppressed $|y_{12}^d|$ and $|y_{21}^d|$, as indicated in previous works (T. T. Hong *et al.*, 2024).

For the free parameters of the 2HDMN_{L,R} model, the numerical scanning ranges are chosen in general as follows

$$\begin{aligned} m_{n_2} &\in [0.051, 0.0525] \text{ eV}; M_0, m_{c_{1,2}} \in [1, 10] \text{ TeV}; \\ \lambda_1, |\lambda_4|, |\lambda_5| &\in [0, 4\pi]; t_\beta \in [5, 30]; \\ x_0 &\in [10^{-5}, 5 \times 10^{-4}]; \phi \in [0, \pi]; \\ |y_{ab}^d| &\leq 3.5 \forall a, b = 1, 2, 3. \end{aligned} \quad (14)$$

In the numerical investigation, we remind all Yukawa and Higgs self couplings must satisfy additional conditions of perturbative limits and Higgs potential constraints indicated precisely in (T. T. Hong *et al.*, 2024).

Firstly, we consider the simplest case that only two entries of y_{ab}^d are non-zeros, which are enough to accommodate two $(g-2)_{e,\mu}$ data, namely $y_{11}^d, y_{22}^d \neq 0$. This case nearly satisfies the experimental constraints of cLFV decays $\text{Br}(e_b \rightarrow e_a \gamma)$, namely, the experimental constraint from $\text{Br}(\mu \rightarrow e\gamma)$ gives strictly allowed regions of parameter space, especially when it combines with two allowed 1σ ranges of $(g-2)_{e,\mu}$. We confirm that all results are consistent with the conclusion given in (T. T. Hong *et al.*, 2024), even when m_{n_2} changes in the allowed ranges. The numerical illustrations is shown in Fig. 2, where just focus on the dependence of all $(g-2)_{e,\mu}$ and LFV decay on m_{n_2} . We emphasize that this dependence was not shown in previous

work. We list here some allowed ranges of parameters that are more strict than the general scanning ranges given in Eq.(14):

$$t_\beta \leq 13.6; 0.02 \leq |y_{11}^d| \leq 0.12, 0.99 \leq |y_{22}^d| \leq 2.5. \quad (15)$$

In addition, the upper bounds of LFV decay rates are predicted to be suppressed when comparing with the future sensitivities given in Table 1: $\text{Br}(\tau \rightarrow e\gamma) < 4 \times 10^{-14}$, $\text{Br}(\tau \rightarrow \mu\gamma) < 10^{-12}$, $\text{Br}(h \rightarrow \mu e) < 1.2 \times 10^{-9}$, $\text{Br}(h \rightarrow \tau e) < 3 \times 10^{-7}$, and $\text{Br}(h \rightarrow \tau\mu) < 7.4 \times 10^{-6}$. On the other hand, the LFVZ decay rate is large enough to reach the expected sensitivities: $\text{Br}(Z \rightarrow \mu e) < 1.2 \times 10^{-7}$, $\text{Br}(Z \rightarrow \tau e) < 2.1 \times 10^{-9}$, $\text{Br}(Z \rightarrow \tau\mu) < 5.3 \times 10^{-8}$.

The second numerical results will focus on the regions with non-zero y_{ab}^d : $0 \leq |y_{ab}^d| \leq 0.5$ for all $(ab) \neq (11), (22), (12), (21)$. Different from the code used in (T. T. Hong *et al.*, 2024), some interesting numerical results are discussed as follows. Fig. 3 shows also the dependence of all mentioned LFV decays on m_{n_2} . It is shown that all cLFV decays $e_b \rightarrow e_a \gamma$ can reach the present constraints from experiments given in Table 1. The maximal values of LFVh and LFVZ decay rates predicted in this case are:

$$\begin{aligned} \text{Br}(Z \rightarrow \mu^\pm e^\mp) &\leq 4.12 \times 10^{-8}, \text{Br}(Z \rightarrow \tau^\pm e^\mp) \leq 2.08 \times 10^{-8}, \\ \text{Br}(Z \rightarrow \tau^\pm \mu^\mp) &\leq 6.49 \times 10^{-6}, \text{Br}(h \rightarrow \mu e) \leq 2.6 \times 10^{-11}, \\ \text{Br}(h \rightarrow \tau e) &\leq 1.8 \times 10^{-3}, \text{Br}(h \rightarrow \tau\mu) \leq 1.5 \times 10^{-3}. \end{aligned} \quad (16)$$

This also means that only the LFVh decay $h \rightarrow \mu e$ is still invisible in the incoming experimental sensitivities listed in Table 1. To end this section, we conclude that our results are consistent with those discussed in (T. T. Hong *et al.*, 2024) in all allowed ranges of m_{n_2} . Furthermore, the LFV decay rates do not depend strongly on m_{n_2} .

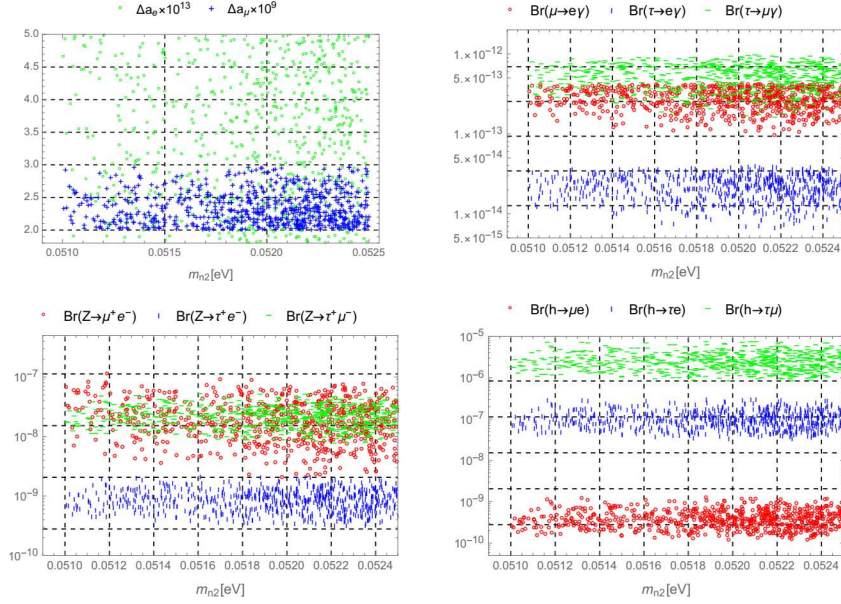


Figure 2. $(g - 2)_{e,\mu}$ anomalies and LFV decays as functions of m_{n2} in the simplest case of only $y_{11}^d, y_{22}^d \neq 0$.

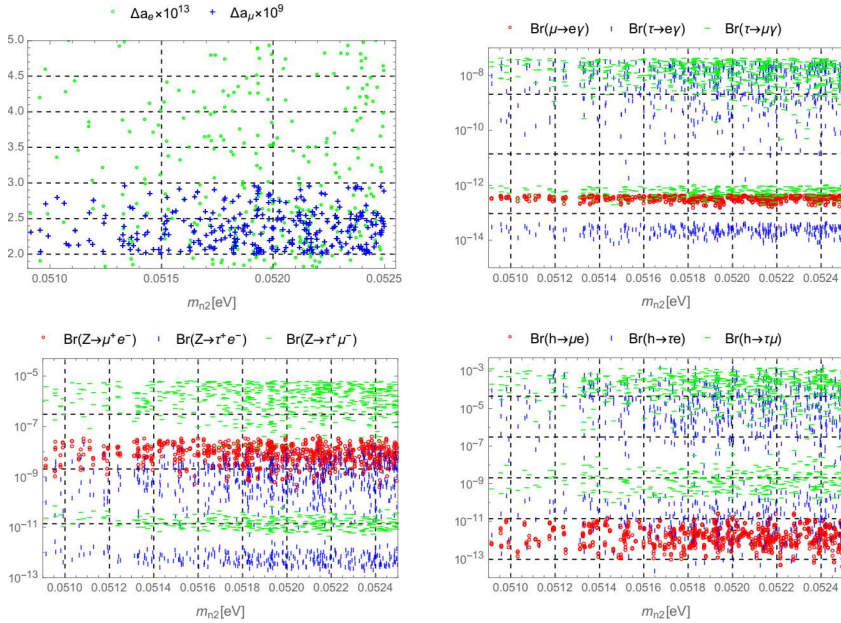


Figure 3. $(g - 2)_{e,\mu}$ anomalies and LFV decays as functions of m_{n2} in the general ranges of $y_{ab}^d \neq 0$ with two non-zero entries $(ab) \neq (12), (21)$.

4 CONCLUSIONS

In this work we investigate the allowed parameter space satisfying all experimental data of neutrino oscillation, LFV decays of h , Z , and charged leptons, and $(g - 2)_{e,\mu}$ anomalies. Different from (T. T. Hong *et al.*, 2024) that paid attention to the NO scheme of neutrino oscillation data, our results fo-

cus on the IO scheme with all allowed ranges of the heaviest active neutrino masses. We have shown that the two schemes IO and NO predict the same results of LFV decay rates. In addition, they do not depend strongly on the particular values of heaviest active neutrino masses.

ACKNOWLEDGMENTS

We would like to thank Dr. Le Tho Hue for his helpful comments.

REFERENCES

- Aad, G. et al. [ATLAS] (2020). *Search for the decays of the Higgs boson $H \rightarrow ee$ and $H \rightarrow e\mu$ in pp collisions at $\sqrt{s} = 13$ TeV with the ATLAS detector*, Phys. Lett. B **801**, 135148. doi.org/10.1016/j.physletb.2019.135148
- Aad, G. et al. [ATLAS] (2022). *Search for lepton-flavor-violation in Z -boson decays with τ -leptons with the ATLAS detector*, Phys. Rev. Lett. **127**, 271801. doi:10.1103/PhysRevLett.127.271801
- Aad, G. et al. [ATLAS] (2023). *Search for the charged-lepton-flavor-violating decay $Z \rightarrow e\mu$ in pp collisions at $\sqrt{s} = 13$ TeV with the ATLAS detector*, Phys. Rev. D **108**, 032015. doi:10.1103/PhysRevD.108.032015
- Abada, A. et al. [FCC], (2019). *FCC Physics Opportunities: Future Circular Collider Conceptual Design Report Volume 1*, Eur. Phys. J. C **79**, no.6, 474. doi:10.1140/epjc/s10052-019-6904-3
- Abdesselam, A. et al. [Belle] (2021). *Search for lepton-flavor-violating tau-lepton decays to $\ell\gamma$ at Belle*, JHEP **10**, 19. doi:10.1007/JHEP10(2021)019
- Aghanim, N. et al. [Planck] (2020). *Planck 2018 results. VI. Cosmological parameters*, Astron. Astrophys. **641**, A6 [erratum: Astron. Astrophys. **652** (2021), C4]. doi:10.1051/0004-6361/201833910
- Aguillard, D. P. et al. [Muon g-2] (2023). *Measurement of the Positive Muon Anomalous Magnetic Moment to 0.20 ppm*, Phys. Rev. Lett. **131**, no.16, 161802. doi:10.1103/PhysRevLett.131.161802
- Altmannshofer, W. et al. [Belle-II] (2020). *The Belle II Physics Book*, PTEP **2019** (2019) no.12, 123C01 [erratum: PTEP **2020**, no.2, 029201]. doi:10.1093/ptep/ptz106
- Aoki, M., Kanemura, S., Takeuchi, M., Zamakhsyari, L. (2023). *Probing the chirality structure in the lepton-flavor-violating Higgs decay $h \rightarrow \tau\mu$ at the LHC*, Phys. Rev. D **107**, no.5, 055037. doi:10.1103/PhysRevD.107.055037
- Aoyama, T. et al. (2020). *The anomalous magnetic moment of the muon in the Standard Model*, Phys. Rept. **887**, 1-166. doi:10.1016/j.physrep.2020.07.006
- Aubert, Bernard et al. [BaBar] (2010). *Searches for Lepton Flavor Violation in the Decays $\tau^\pm \rightarrow e^\pm\gamma$ and $\tau^\pm \rightarrow \mu^\pm\gamma$* , Phys. Rev. Lett. **104**, 021802. doi:10.1103/PhysRevLett.104.021802
- Baldini, A. M. et al. [MEG] (2016). *Search for the lepton flavour violating decay $\mu^+ \rightarrow e^+\gamma$ with the full dataset of the MEG experiment*, Eur. Phys. J. C **76**, no.8, 434. doi:10.1140/epjc/s10052-016-4271-x
- Baldini, A. M. et al. [MEG II] (2018). *The design of the MEG II experiment*, Eur. Phys. J. C **78**, no.5, 380. doi:10.1140/epjc/s10052-018-5845-6
- Barman, R. K., Dev, P. S. B., Thapa, A. (2023). *Constraining lepton flavor violating Higgs couplings at the HL-LHC in the vector boson fusion channel*, Phys. Rev. D **107** no.7, 075018. doi:10.1103/PhysRevD.107.075018
- Branco, G. C., Ferreira, P. M., Lavoura, L., Rebelo, M. N., Sher, Marc, Silva, Joao P. (2012). *Theory and phenomenology of two-Higgs-doublet models*, Phys. Rept. **516**, 1-102. doi:10.1016/j.physrep.2012.02.002
- Crivellin, A., Hoferichter M., Schmidt-Wellenburg, P. (2018). *Combined explanations of $(g-2)_{\mu,e}$ and implications for a large muon EDM*, Phys. Rev. D **98**, no.11, 113002. doi:10.1103/PhysRevD.98.113002
- Dam, M. (2019). *Tau-lepton Physics at the FCC-ee circular e^+e^- Collider*, SciPost Phys. Proc. **1**, 041. doi:10.21468/SciPostPhysProc.1.041
- Fan, X., Myers, T. G., Sukra, B. A. D., Gabrielse, G. (2023). *Measurement of the Electron Magnetic Moment*, Phys. Rev. Lett. **130**, no.7, 071801. doi:10.1103/PhysRevLett.130.071801
- Hong, T. T., Tran, Q. Duyet, Nguyen, T. Phong, Hue, L. T., Nha, N. H. T. (2024). *$(g-2)_{e,\mu}$ anomalies and decays $h \rightarrow e_a e_b$, $Z \rightarrow e_a e_b$, and $e_b \rightarrow e_a \gamma$ in a two Higgs doublet model with inverse seesaw neutrinos*, Eur. Phys. J. C **84**, no.3, 338 [erratum: Eur. Phys. J. C **84**, no.5, 454 (2024)]. doi:10.1140/epjc/s10052-024-12692-y
- Hue, L. T., Cárcamo Hernández, A. E., Long, H. N., Hong, T. T. (2022). *Heavy singly charged Higgs bosons and inverse seesaw neutrinos as origins of large $(g-2)_{e,\mu}$ in two Higgs doublet models*, Nucl. Phys. B **984**, 115962. doi:10.1016/j.nuclphysb.2022.115962
- Hue, L. T., Long, H. N., Binh, V. H., Mai, H. L. T., Nguyen, T. P. (2023). *One-loop contribu-*

- tions to decays $e_b \rightarrow e_a \gamma$ and $(g - 2)_{e_a}$ anomalies, and Ward identity, Nucl. Phys. B **992**, 116244. doi:10.1016/j.nuclphysb.2023.116244
- Hue, L. T., Ninh, L. D., Thuc, T. T., Dat, N. T. T. (2018). Exact one-loop results for $l_i \rightarrow l_j \gamma$ in 3-3-1 models, Eur. Phys. J. C **78**, no.2, 128. doi:10.1140/epjc/s10052-018-5589-3
- Lavoura, L. (2003). General formulae for $f_1 \rightarrow f_2 \gamma$, Eur. Phys. J. C **29**, 191-195. doi:10.1140/epjc/s2003-01212-7
- Mondal, T., Okada, H. (2022). Inverse seesaw and $(g - 2)$ anomalies in $B - L$ extended two Higgs doublet model, Nucl. Phys. B **976**, 115716.
- Qin, Q., Li, Q., Lü, C. D., Yu, F. S., Zhou, S. H. (2018). Charged lepton flavor violating Higgs decays at future e^+e^- colliders, Eur. Phys. J. C **78**, no.10, 835. doi:10.1140/epjc/s10052-018-6298-7
- Sirunyan, A. M. et al. [CMS] (2021). Search for lepton-flavor violating decays of the Higgs boson in the $\mu\tau$ and $e\tau$ final states in proton-proton collisions at $\sqrt{s} = 13$ TeV, Phys. Rev. D **104**, no.3, 032013. doi:10.1103/PhysRevD.104.032013
- Workman, R. L. et al. [Particle Data Group] (2022). Review of Particle Physics, PTEP **2022**, 083C01. doi:10.1093/ptep/ptac097